1521-009X/43/7/944–950$25.00
Drug Metabolism and Disposition
http://dx.doi.org/10.1124/dmd.114.061705
Drug Metab Dispos 43:944–950, July 2015

Multidrug Resistance-Associated Protein 3 Plays an Important Role in Protection against Acute Toxicity of Diclofenac [S]

Renato J. Scialis, Iván L. Csanaky, Michael J. Goedken, and José E. Manautou

University of Connecticut, School of Pharmacy, Department of Pharmaceutical Sciences, Storrs, Connecticut (R.J.S., J.E.M.); University of Kansas Medical Center, Department of Internal Medicine, Kansas City, Kansas (I.L.C.); and Office of Translational Science, Rutgers University, Piscataway, New Jersey (M.J.G.)

Received October 27, 2014; accepted April 20, 2015

ABSTRACT

Diclofenac (DCF) is a nonsteroidal anti-inflammatory drug commonly prescribed to reduce pain in acute and chronic inflammatory diseases. One of the main DCF metabolites is a reactive diclofenac acyl glucuronide (DCF-AG) that covalently binds to biologic targets and may contribute to adverse drug reactions arising from DCF use. Cellular efflux of DCF-AG is partially mediated by multidrug resistance-associated proteins (Mrp). The importance of Mrp2 during DCF-induced toxicity has been established, yet the role of Mrp3 remains largely unexplored. In the present work, Mrp3-null (KO) mice were used to study the toxicokinetics and toxicodynamics of DCF and its metabolites. DCF-AG plasma concentrations were 90% lower in KO mice than in wild-type (WT) mice, indicating that Mrp3 mediates DCF-AG basolateral efflux. In contrast, there were no differences in DCF-AG biliary excretion between WT and KO, suggesting that only DCF-AG basolateral efflux is compromised by Mrp3 deletion. Susceptibility to toxicity was also evaluated after a single high DCF dose. No signs of injury were detected in livers and kidneys; however, ulcers were found in the small intestines. Furthermore, the observed intestinal injuries were consistently more severe in KO compared with WT. DCF covalent adducts were observed in liver and small intestines; however, staining intensity did not correlate with the severity of injuries, implying that tissues respond differently to covalent modification. Overall, the data provide strong evidence that (1) in vivo Mrp3 plays an important role in DCF-AG disposition and (2) compromised Mrp3 function can enhance injury in the gastrointestinal tract after DCF treatment.

Introduction

Diclofenac (DCF) is a nonsteroidal anti-inflammatory drug (NSAID) that is prescribed to alleviate symptoms associated with ankylosing spondylitis, osteoarthritis, rheumatoid arthritis, and migraine (McNeely and Goa, 1999; Depomed, 2009; Novartis, 2011). DCF is generally well tolerated, although long-term usage has been implicated with a variety of adverse events in a subset of patients. The most common side effects of DCF are discomfort, ulceration, and bleeding in the gastrointestinal (GI) tract. These adverse events are related to DCF pharmacodynamics, namely chronic inhibition of cyclooxygenase (COX) enzymes causing a decrease of prostaglandins that protect the GI mucosa (Menasse et al., 1978; Wallace, 2008). NSAIDs as a group have a mean liver injury rate of 1 per 100,000 users. However, chronic DCF administration increases the risk of liver injury to 6 per 100,000 users (de Abajo et al., 2004). More recently, a meta-analysis of cardiovascular safety implicated DCF with a higher risk of cardiovascular death and stroke among a group of seven NSAIDs (Trelle et al., 2011).

DCF undergoes extensive first-pass metabolism in humans, and approximately 50% of the dose is systemically available (Willis et al., 1979). The majority of DCF is converted into metabolites, of which 65% are eliminated in urine with the remainder excreted in bile (Riess et al., 1978; Novartis, 2011). Among the main products are hydroxylated metabolites, the predominant being 4′-hydroxy diclofenac (OH-DCF), that can form reactive quinoneimines that adduct and deplete glutathione causing a state of oxidative stress (Tang et al., 1999). Another key metabolite is the highly reactive diclofenac acyl glucuronide (DCF-AG), which is primarily catalyzed in humans by uridine 5′-diphospho-glucuronosyltransferase (UGT) 2B7 (King et al., 2001). It has been shown that inheritance of one or two copies of the UGT2B7*2 allele was associated with an increased risk of DCF-induced hepatotoxicity compared with UGT2B7*1 homozygotes because the *2 variant possesses higher catalytic activity (Daly et al., 2007).

DCF-AG is initially formed as a β-1-*O*-acyl glucuronide (β-anomer), which can be cleaved by β-glucuronidase into DCF and glucuronic acid. β-Anomers spontaneously isomerize into β-glucuronidase-resistant 2-, 3-, and 4-*O*-acyl isomers (Sallustio et al., 2000). DCF-AG undergoes these rearrangements as the pH changes from acidic to physiologic conditions such as those that occur in the GI tract (Ebner et al., 1999; Kenny et al., 2004). DCF-AG can form adducts with multiple proteins in the liver and GI tract, and dipeptidyl peptidase IV was identified as a DCF-AG target in rat liver, where adduction resulted in decreased activity (Hargus et al., 1995). Furthermore, it was found that broad-acting UGT inhibitors can significantly diminish the covalent binding of DCF metabolite to hepatocellular proteins in vitro (Kretz-Rommel and

This work was supported by the National Institutes of Health [Grant DK069557].
dx.doi.org/10.1124/dmd.114.061705.
[S] This article has supplemental material available at dmd.aspetjournals.org.

ABBREVIATIONS: ALT, alanine aminotransferase; Bcrp, breast cancer resistance protein; BUN, blood urea nitrogen; COX, cyclooxygenases; DCF, diclofenac; DCF-AG, diclofenac acyl glucuronide; DPBS, Dulbecco's phosphate buffered saline; GI, gastrointestinal; KO, knockout; LC/MS/MS, tandem liquid chromatography mass spectrometry; MRP, multidrug resistance-associated protein; NSAID, nonsteroidal anti-inflammatory drug; OATP, organic anion transporting polypeptide; OH-DCF, 4′-hydroxy diclofenac; SNP, single nucleotide polymorphism; UGT, uridine 5′-diphospho-glucuronosyltransferase; WT, wild type.

Boelsterli, 1993). There is consensus that repeated exposure to DCF-AG contributes to the idiosyncratic drug reaction seen with clinical usage; however, the exact nature of how DCF-AG contributes to these idiosyncracies remains unclear.

The potential for DCF-AG to cause extrahepatic covalent binding modifications is contingent upon active transport. For instance, DCF-AG was not detected in the bile of rats lacking canalicular multidrug resistance-associated protein 2/ATP-binding cassette transporter family c2 (Mrp2/Abcc2) (Seitz et al., 1998). A follow-up study revealed that Mrp2-null rats also had reduced intestinal ulceration compared with WT rats (Seitz and Boelsterli, 1998). These findings are important because they suggest that Mrp2 is at least partially responsible for DCF-AG excretion from hepatocytes into bile. The mechanism by which DCF-AG is transported from hepatocytes into blood remains less understood.

Among the MRPs that are expressed along the basolateral membrane, MRP3 (ATP-binding cassette transporter family C3) has been demonstrated to export glucuronide conjugates of other compounds (Zelcer et al., 2001, 2006). In a Caucasian sample pool, 51 single nucleotide polymorphisms (SNP) in MRP3 were found (Lang et al., 2004). A pharmacogenomic study of healthy Japanese subjects identified 21 novel SNPs, with two resulting in immature transcript due to insertion of a stop codon (Fukushima-Uesaka et al., 2007). Functional significance of MRP3 SNPs was demonstrated whereby several MRP3 SNPs expressed in an in vitro system had impaired transporter function either by reduction in transporter activity or disruption of intracellular transporter trafficking to the cell membrane (Kobayashi et al., 2008).

Because MRP3 has been shown to transport both endogenous and exogenous glucuronide conjugates, it can be hypothesized that perturbation of MRP3 expression or function may affect the disposition and toxicity of DCF-AG in vivo. To investigate the role of MRP3 in the disposition and toxicity of DCF, a mouse Mrp3-null model is used to assess the disposition of DCF-AG and whether Mrp3 deletion increases likelihood of injury.

Materials and Methods

Chemicals, Reagents, and Animals

DCF, OH-DCF, Dulbecco's phosphate buffered saline (DPBS), formic acid, indomethacin, and sodium citrate were purchased from Sigma-Aldrich Corporation (St. Louis, MO). DCF-AG was purchased from Toronto Research Chemicals Incorporated (Toronto, ON, Canada). Solutol HS 15 was provided by the BASF Corporation (Florham Park, NJ). DCF antiserum was graciously donated by Dr. Dietmar Knopp (Technische Universität München, München, Germany). Mrp3-null mice of FVB 129/Ola background were provided by Dr. Piet Borst (Netherlands Cancer Institute, Amsterdam, Netherlands). An additional set of Mrp3-null mice having C57BL/6J background were generated at the University of Kansas Medical Center. Mice were housed in an American Animal Associations Laboratory Animal Care accredited facility of University of Kansas Medical Center under a standard temperature-, light-, and humidity-controlled environment. Mice had free access to Laboratory Rodent Chow 8604 (Harlan, Madison, WI) and drinking water. All animal studies were performed in accordance with the Guide for the Care and Use of Laboratory Animals using protocols reviewed and approved by the local Institutional Animal Care and Use Committee of University of Kansas Medical Center (Kansas City, KS).

In Vivo Studies

Toxicokinetics. Male 2- to 3-month-old FVB 129/Ola WT and FVB 129/Ola KO mice were anesthetized intraperitoneally with a ketamine/midazolam mixture (100 and 5 mg/kg, respectively), and both the right carotid artery and the common bile duct were cannulated for sample collection. The mice received a single intra-arterial dose of 75 mg/kg DCF in 10:90 (v/v) Solutol HS 15:DPBS at a dosing volume of 5 ml/kg. Bile flow was monitored, and bile fractions were collected in 15-minute intervals from −15 to 0, 0 to 15, 15 to 30, 30 to 45, 45 to 60, 60 to 75, and 75 to 90 minutes postadministration. Blood samples were collected into heparinized tubes at 2, 7.5, 22.5, 37.5, 52.5, 67.5, and 90 minutes after administration, and the blood was subsequently centrifuged to yield plasma. The volumes of bile were determined gravimetrically using 1.0 for specific gravity. Both bile and plasma were stored at −20°C until analysis. At the conclusion of the study (90-minute postadministration), animals were killed by overdose with ketamine and midazolam. Livers were harvested and quickly frozen in liquid nitrogen prior to storage at −80°C.

Toxicodynamics. Two- to three-month-old male WT and KO (C57BL/6 background) were injected a single intraperitoneal dose of either vehicle, 10:90 (v/v) Solutol HS15: DPBS, or 90 mg/kg DCF in vehicle at a dosing volume of 5 ml/kg. The mice were then allowed access to food and water ad libitum. Twenty four hours after dosing, the mice were anesthetized for sacrifice with an intraperitoneal injection of 50 to 70 mg/kg pentobarbital. Blood was collected and centrifuged to yield plasma and kept frozen at −20°C. Kidneys, liver, and small intestines were harvested, fixed in buffered formalin for 24 hours with gentle shaking at room temperature, and then transferred into 70% ethanol. Tissues were subsequently paraffin embedded and sectioned onto glass slides for histopathology and immunohistochemistry.

Bioanalytical Analysis

Sample Treatment. Bile and plasma were diluted with 0.1% formic acid in water (Solvent A) for tandem liquid chromatography mass spectrometry (LC/MS/MS) detection as well as to stabilize DCF-AG. Liver samples were homogenized by bead milling using Solvent A. A 50-μl aliquot of diluted biologic matrix was then precipitated with 450 μl of 0.1% formic acid in acetonitrile (Solvent B) containing indomethacin as an internal standard. Standard curves using naive matrices were prepared in a similar fashion. Samples and standards were vigorously vortex mixed and centrifuged at 1350 *g* for 10 minutes and 4°C. A 200-μl aliquot of supernatant was removed and evaporated under nitrogen gas at 45°C. The resulting residue was reconstituted with 200 μl of 90:10 (v/v) A:B, vigorously vortex mixed, and centrifuged before injection onto LC/MS/MS. The injection volume for all sample types was 10 μl.

LC/MS/MS Method. Chromatographic separation of analytes was performed on a Synergi 4 μm Max-RP 80 Å 50 × 2 mm column (Phenomenex Incorporated, Torrance, CA). The system front end consisted of an HTC PAL Autosampler outfitted with a Coolstack set to 4°C (LEAP Technologies Incorporated, Carrboro, NC), an SCL-10Avp system controller, two LC10ADvp pumps, and a DGU-14A degasser (Shimadzu Scientific Instruments, Columbia, MD). Analytes of interest were eluted using a gradient profile that began with 10% solvent B for the first 1.0 minute, which was then increased to 90% solvent B at 3.5 minutes using a linear gradient and held at this mixture for 0.5 minute before reverting back to initial solvent conditions for 1.0 minute to re-equilibrate the column. The flow rate was 0.4 ml/min, and the column effluent was directed to waste for the initial 1.5 minutes before switching to the mass spectrometer. Analytes were detected using an AB Sciex API 4000 LC/MS/MS triple quad mass-spectrometer with a TurboIonSpray probe and Analyst version 1.4.2 software (AB Sciex, Framingham, MA) that was operated in multiple reaction monitoring mode. Ion spray voltage was −4250 V, and the source temperature was set to 400°C. The mass transitions in negative ion mode for monitoring DCF, OH-DCF, DCF-AG, and indomethacin were *m/z* 294.0→249.9, 309.9→265.9, 470.1→192.9, and 356.0→311.8, respectively. The retention times of diclofenac, 4′-hydroxy diclofenac, diclofenac acyl glucuronide, and indomethacin were 3.25, 2.84, 2.69, and 3.20 minutes, respectively. Concentrations of analytes in the samples were determined by comparing the peak area ratios (analyte/internal standard) to those in the standard curve using a linear regression model. The dynamic range was 10 to 5,000 ng/ml for bile, liver homogenate, and plasma samples. The criterion of acceptance for standards was defined to be ±20% of nominal concentration.

Immunohistochemistry

Slides for immunohistochemistry were deparaffinized by xylene, and the xylene was removed by sequentially decreasing concentrations of ethanol followed by hydration in water. After a 30-minute heat-induced epitope retrieval in sodium citrate buffer, endogenous peroxidase activity was blocked with 3% hydrogen peroxide for 15 minutes. Slides were subsequently treated with an Avidin/Biotin Blocking Kit (Vector Laboratories Incorporated, Burlingame, CA) as per the manufacturer's recommendations and incubated with a Dako Serum-free Protein

Block (Dako Incorporated, Carpinteria, CA) for 30 minutes. A rabbit polyclonal primary antibody against DCF at a 1:5000 dilution was applied for 60 minutes at room temperature, after which slides were incubated for 30 minutes with a 1:300 dilution of a Dako biotinylated swine anti-rabbit secondary antibody. The slides were then exposed to streptavidin-horseradish peroxidase (BD Biosciences, San Jose, CA) for 30 minutes. To develop the chromagen, a 30-minute treatment with a Vector NovaRED Substrate Kit was used, and slides were counterstained with Mayer's Hematoxylin (Life Technologies, Grand Island, NY). Finally, slides were dehydrated with ethanol and xylene and placed under a coverslip using Histomount Mounting Solution (Life Technologies). For negative controls, samples from the vehicle-only groups were treated in the same manner as subjects dosed with DCF.

Clinical Chemistry

Plasma samples from the toxicodynamic study were analyzed for alanine aminotransferase (ALT) and blood urea nitrogen (BUN) using kits purchased from Thermo Fisher Scientific Incorporated (Waltham, MA) as per the manufacturer's recommendations. Positive and negative controls were used to assess assay functionality. A BioTek UV/Vis microplate spectrophotometer (BioTek Instruments Incorporated, Winooski, VT) was used to measure assay endpoints.

Histopathology

Liver and Kidney. Liver and kidney samples were fixed in 10% neutral-buffered zinc formalin before processing and paraffin embedding. Tissue sections (5 μm) were stained with hematoxylin and eosin. Sections were examined by light microscopy for the presence and severity of necrosis and degeneration using an established grading system (Manautou et al., 1994).

Gastrointestinal Tract. The gastrointestinal tract was examined histologically with multiple transverse sections of the stomach and large intestine and Swiss Roll sections of the small intestine (Moolenbeek and Ruitenberg, 1981). Histologic examination used a scoring system adapted from a method described by Krieglstein et al. (2007). Briefly, three independent parameters were measured for a combined semiquantitative injury score: the degree of villus/crypt damage, the severity of inflammation (none, minimal, mild, moderate, marked, and severe), and the depth of injury (mucosa with epithelium and lamina propria, submucosa, muscularis, and serosa).

Statistical Analysis

Data are expressed as mean ± standard error of the mean. P values ≤ 0.05 were considered as statistically significant. GraphPad Prism version 6.0 (GraphPad Software Incorporated, La Jolla, CA) was used for statistical analysis of data. Two groups were compared by Student's t test. Multiple groups were compared by an analysis of variance followed by Newman-Keuls post hoc test.

Results

Toxicokinetic Study. In animals that remained anesthetized for surgical exposure of the abdominal cavity and bile duct cannulation, the maximal tolerated dose without morbidity was 75 mg/kg. Plasma concentrations for 75 mg/kg DCF (Fig. 1A) were significantly higher in KO compared with WT, and the increases were generally less than 40%. Conversely, OH-DCF concentrations in plasma (Fig. 1B) were significantly higher in WT with a 90% increase observed at 37.5 minutes. There was a dramatic disparity in plasma concentrations between WT and KO for DCF-AG (Fig. 1C), with WT having nearly ninefold higher concentrations in plasma compared with KO. A summary of pertinent toxicokinetic parameters is presented in Table 1. Both genotypes had similar estimated DCF plasma concentrations at time zero. Although there was a difference in the DCF elimination half-life between the two genotypes, the DCF plasma exposure for WT and KO was comparable.

To determine whether the loss of Mrp3 affected the biliary disposition of DCF and the two metabolites under consideration, the biliary excretion of DCF and its metabolites were quantified. There was no difference in bile flow between WT and KO (data not shown). The biliary excretions of DCF and its metabolites were comparable between the two genotypes (Fig. 1, D, E, and F). Of the three analytes, DCF-AG was most predominant in bile, constituting nearly 10% of the total DCF dose for each genotype, whereas DCF and OH-DCF biliary concentrations accounted for 0.2 and 0.1% of total DCF dose, respectively,

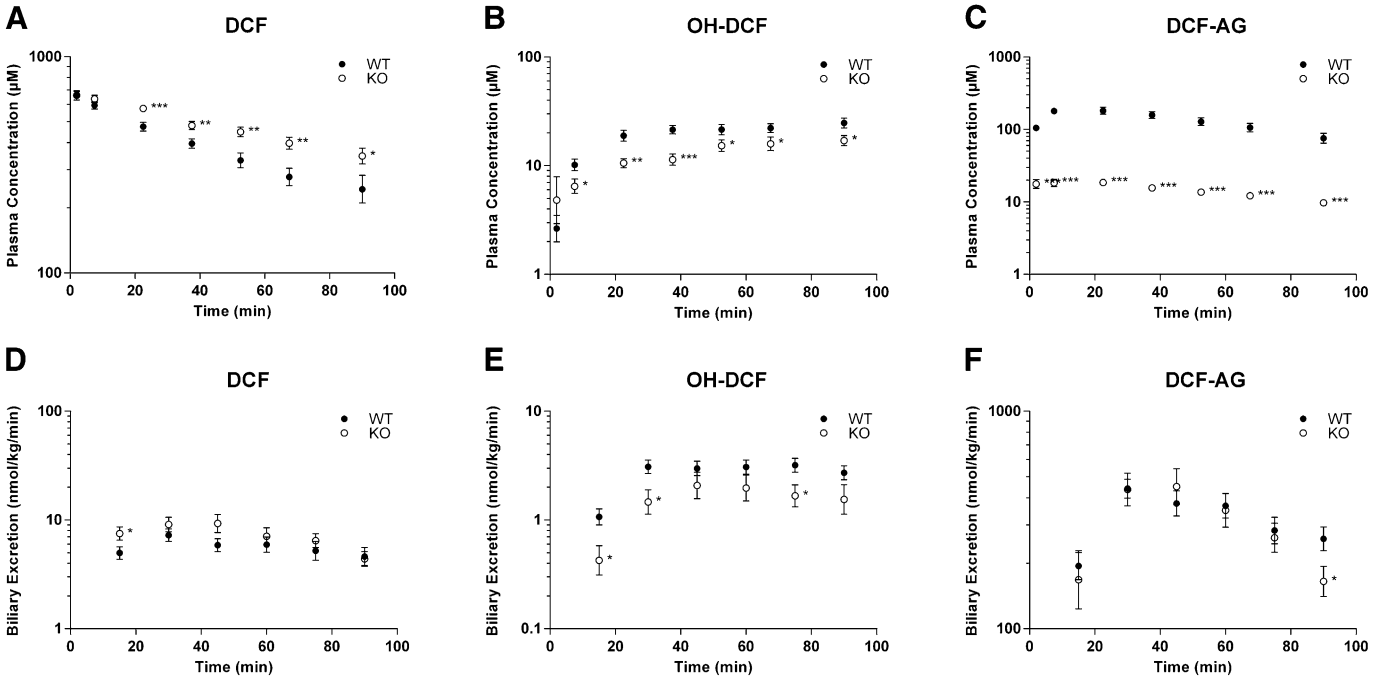

Fig. 1. Toxicokinetics of DCF and its metabolites in FVB wild-type (WT, ●) and FVB Mrp3-null (KO, ○) mice after a single intra-arterial dose of 75 mg/kg DCF. (A–C) Plasma concentration profiles for DCF (A), OH-DCF (B), and DCF-AG (C) at discrete time points. (D–F) Biliary excretion profiles for DCF (D), OH-DCF (E), and DCF-AG (F). Time points represent biliary excretion during successive 15-minute intervals (0–15, 15–30, 30–45, 45–60, 60–75, and 75–90 minutes). All data are expressed as mean ± standard error of the mean for 10–12 subjects/group. *$P < 0.05$; **$P < 0.01$; ***$P < 0.001$ versus WT.

TABLE 1

Summary of DCF toxicokinetic parameters in plasma of FVB WT and FVB Mrp3-null after a single 75 mg/kg DCF dose

Data are expressed as mean ± S.E. of the mean for 10–12 subjects/group.

Group	C_0	$t_{1/2}$	$AUC_{0\text{-tlast}}$
	μM	*min*	$\mu M \times min$
WT	699 ± 31	74.1 ± 12.8	34,600 ± 2,100
KO	701 ± 38	108 ± 10	35,900 ± 2,500

C_0, indicates the estimated DCF plasma concentration at time zero; $t_{1/2}$, DCF elimination half-life; $AUC_{0\text{-tlast}}$, area under the plasma concentration versus time curve for DCF from time zero to the last collected time point.

irrespective of genotype. The limited availability of KO mice permitted assessing hepatic concentrations of DCF and its metabolites only at the terminal time point of 90 minutes postadministration. The KO livers had more DCF, although the difference was not statistically significant. OH-DCF and DCF-AG concentrations in KO livers were statistically lower compared with WT (Fig. 2). In contrast to bile, for which the major detected analyte was DCF-AG, unchanged DCF in both genotypes was most abundant compared with OH-DCF and DCF-AG.

Clinical Chemistry. Having established a role for Mrp3 to modulate systemic exposure of DCF-AG in vivo, the next objective was to evaluate to susceptibility of KO to DCF-induced injury. For these studies, the DCF dose was increased to 90 mg/kg because that was the maximal nonlethal dose in animals that underwent no surgery and were freely moving. Rather than oral gavage, intraperitoneal administration was used to maximize dose absorption and delivery of DCF via portal circulation for immediate uptake into the liver. ALT concentrations (Fig. 3A) were not significantly different between WT and KO, indicating lack of injury in the liver. Furthermore, ALT values in all vehicle control and DCF-treated groups were less than 30 U/l, which is within the upper limit of normal range for ALT. BUN levels (Fig. 3B) were statistically higher in KO mice compared with WT; however, the lack of difference between vehicle- and DCF-treated groups in KO mice suggest there was no DCF-induced renal injury.

Histopathology. Histopathological examination of liver and kidneys showed no obvious injuries at the administered dose, confirming the clinical chemistry results (data not shown). The small intestines were also examined and scored according to three categories of injury. WT mice that received DCF showed a trend of higher injury compared with vehicle-treated mice (Fig. 4), although these differences were not statistically significant. In addition, KO dosed with DCF had significantly greater incidence and severity of erosions and ulcers compared with treatment-matched WT mice. For both WT and KO mice, ulcers were observed in the jejunal and ileal but not duodenal regions of the small intestine. Thus the data suggest that the loss of Mrp3 increased the susceptibility to intestinal injury from an acute dose of DCF.

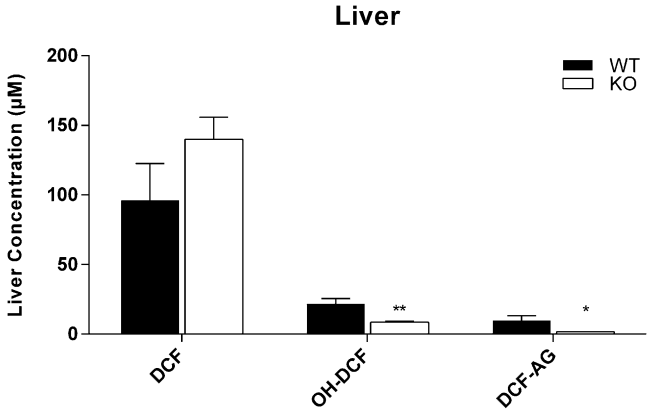

Fig. 2. Hepatic concentrations of DCF, OH-DCF, and DCF-AG in FVB wild-type (WT, ■) and FVB Mrp3-null (KO, □) mice. Mice were injected with 75 mg/kg DCF. Livers were harvested 90 minutes after administration of vehicle or DCF. Data are expressed as mean ± standard error of the mean for 10–12 subjects/group. $*P < 0.05$; $**P < 0.01$ versus WT.

Immunohistochemistry. Sections of livers, kidneys, and small intestines were subjected to immunohistochemistry to determine the extent of DCF adduction. The rationale for conducting this assay was that reactive intermediates or metabolites of DCF are known to covalently bind to proteins. Thus the goal was to establish possible links between covalent binding of reactive DCF products and tissue injury. Kidneys were entirely devoid of DCF adduct staining, implying that reactive DCF metabolites were not likely to be generated or accumulated in kidneys (data not shown). In contrast, WT and KO livers showed strong evidence of DCF adduction after DCF administration compared with vehicle controls. The staining was robust and was observed in centrilobular, midzonal, and periportal regions. Vehicle controls did not exhibit staining, suggesting that the primary antibody was specific for diclofenac adducts (Fig. 5A). Interestingly, the livers showed intense staining for DCF adduct, yet this organ did not manifest any apparent signs of injury either through clinical chemistry or histopathology. Finally, compared with small intestines from vehicle controls, which were unremarkable (Fig. 5D), the small intestines from WT and KO also exhibited positive staining of DCF adducts (Fig. 5, E and F). The level of adduct staining in the small intestine was notably weaker than that observed in the liver as qualitatively assessed by chromagen intensity and the degree of scatter. Adduct formation was detected along the brush border of villi and extended inward toward the basement membrane. In terms of regiospecificity, staining was scattered throughout the small intestine and did not appear to be confined to any particular location.

Discussion

This work explores the role of Mrp3 on the disposition and acute toxicity of DCF. DCF has high passive permeability, therefore its uptake into tissues should not be limited by active transport processes (Huang et al., 2010). The elevated DCF and lower OH-DCF plasma concentrations in KO compared with WT (Fig. 1, A and B) may indicate metabolic saturation. In vitro studies using mouse hepatic S9 fraction did not show differences in DCF metabolism, because the WT and KO K_m values were comparable (data not shown). Further evidence of metabolic saturation comes from the OH-DCF plasma concentration-time profile, which was relatively flat at 75 mg/kg DCF, whereas at lower doses plasma OH-DCF was initially high before decreasing by first-order kinetics (Supplemental Fig. 1).

The present DCF-AG data are consistent with low-dose studies and demonstrate Mrp3-mediated DCF-AG efflux (Fig. 1C). Our data confirm the observation reported by Lagas et al. (2010) that DCF-AG is an in vivo substrate of mouse Mrp3. KO had DCF-AG plasma concentrations that were nearly 90% lower compared with WT. Plasma concentrations of several glucuronide metabolites have been reported to be lower in Mrp3 KO compared with WT mice (Manautou et al., 2005; Zamek-Gliszczynski et al., 2006). Because KO mice were comparable with WT in terms of overall transporter expression except for Mrp3, the results indicate that Mrp3 mediates DCF-AG basolateral efflux in vivo.

DCF, OH-DCF, and DCF-AG biliary excretion showed no evident distinction between WT and KO. Because Mrp3 acts as a basolateral efflux pump for bile acids (Zelcer et al., 2003), the bile flow in WT and KO was measured and found to be equal, suggesting that Mrp3 deletion and DCF treatment did not affect bile flow. That DCF-AG

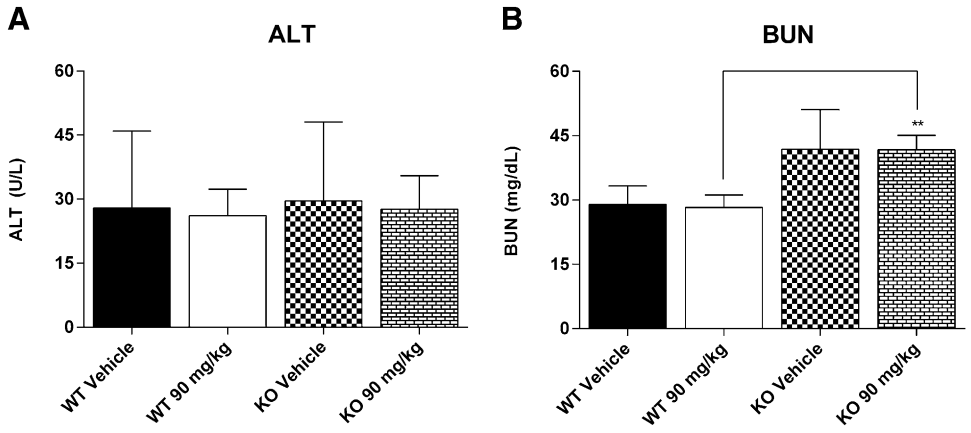

Fig. 3. Clinical chemistry of C57 wild-type (WT) and C57 Mrp3-null (KO) mice 24 hours after a single dose of 90 mg/kg DCF. (A) Plasma alanine aminotransferase (ALT). (B) Plasma blood urea nitrogen (BUN). Results are expressed as mean ± standard error of the mean for 3–7 subjects/group. $^{**}P < 0.01$ versus WT.

biliary excretion was similar between WT and KO was unexpected considering the pronounced plasma differences. Other studies in KO reported that low plasma or perfusate concentrations of glucuronides were inversely correlated with increased glucuronide biliary concentrations compared with WT (Manautou et al., 2005; Zamek-Gliszczynski et al., 2006). Similar to rats, canalicular DCF-AG excretion would likely have been mediated by Mrp2 given the 88% protein sequence homology between mouse and rat Mrp2 (Altschul et al., 2005). Another canalicular transporter, breast cancer resistance protein (Bcrp/Abcg2), has been also demonstrated to transport DCF (Lagas et al., 2009). However, exploratory studies in our laboratory with Bcrp-KO mice resulted in equivalent DCF-AG biliary excretion compared with WT (data not shown).

To account for other possible DCF metabolites, bile fractions were pooled and infused onto the LC/MS/MS for qualitative metabolite profiling. Peaks corresponding to DCF taurine conjugate and hydroxy diclofenac acyl glucuronide were detected (data not shown). Identification of these metabolites is consistent with their formation in rodents (Kenny et al., 2004; Sarda et al., 2012). Nonetheless, the hydroxy diclofenac acyl glucuronide signal in KO bile would not have wholly accounted for the DCF-AG fraction that was diverted from entering the blood. Despite the DCF-AG mass balance inequity between WT and KO, there are instances in which Mrp3 ablation affects basolateral but not canalicular efflux. Zelcer et al. (2006) noted that hyodeoxycholate glucuronide perfusate concentrations were fourfold greater in WT compared with KO, whereas bile concentrations were similar between genotypes. Moreover, fexofenadine plasma concentrations decreased 50% in Mrp3-KO mice relative to WT, yet biliary and hepatic fexofenadine concentrations between the genotypes were the same (Tian et al., 2008). Thus, Mrp3 deletion solely affected DCF-AG basolateral efflux.

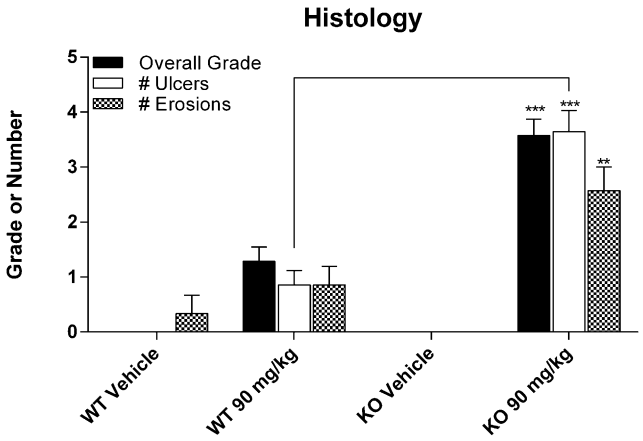

Fig. 4. Summary of histopathology of small intestines from C57 wild-type (WT) and C57 Mrp3-null (KO) mice 24 hours after administration of vehicle or 90 mg/kg DCF. Results are expressed as mean ± standard error of the mean for 3–7 subjects/group. The overall grade was based on the following scheme: 0 = none, 1 = minimal, 2 = mild, 3 = moderate, 4 = marked, and 5 = severe. Ulcers and erosions reflect the number of findings that were identified on an entire tissue section. $^{**}P < 0.01$; $^{***}P < 0.001$ versus treatment-matched WT.

The other aim of this study was to assess the susceptibility of Mrp3-null subjects to DCF-induced injury. Initial studies in FVB 129/Ola mice at a 90 mg/kg DCF dose resulted in KO, but not WT, exhibiting greater intestinal injury (data not shown). Because FVB 129/Ola KO were unavailable, further studies were conducted in C57BL/6 KO. Neither the liver nor kidneys showed any evidence of damage by serum biomarker analysis (Fig. 3). DCF has been shown to induce nephrotoxicity in ICR mice evidenced by a 2.5-fold increase in BUN concentrations 24 hours after an oral 100 mg/kg dose (Hickey et al., 2001). The finding in ICR mice likely reflects that strain's higher sensitivity to renal injury, because C57BL/6 mice (Fig. 3B) had no changes in BUN concentrations compared with vehicle treatment 24 hours after 90 mg/kg intraperitoneal administration. Regarding the liver, Lagas et al. (2010) reported that a 25 mg/kg intraperitoneal DCF injection caused ALT concentrations to increase twofold compared with WT, leading the authors to conclude that slight liver toxicity occurred. However, the mice used in that study were triple knockouts for Bcrp, Mrp2, and Mrp3, making it difficult to ascribe which transporter was truly responsible for enhancing the toxic effect. Additionally, ALT, bilirubin, liver weights, and triglycerides were also slightly elevated in the triple KO versus WT, suggesting that the mice may be more susceptible to challenge by a toxicant (Vlaming et al., 2009). Although liver and kidney were devoid of injury for the present study, the small intestines in both genotypes exhibited damage, with KO mice sustaining greater injury (Fig. 4). The intestinal injury is consistent with published reports on DCF ulcerogenicity (Atchison et al., 2000; Ramirez-Alcantara et al., 2009).

Reactive DCF metabolites form adducts with a number of hepatic proteins (Seitz et al., 1998; Sallustio and Holbrook, 2001; Kenny et al., 2004). Immunohistochemistry revealed widespread covalent binding in the liver and small intestine but not in kidneys of both WT and KO (Fig. 5). Qualitative assessment of the extent of staining did not provide meaningful distinction between the two genotypes (data not shown). DCF adduct staining was most intense in the liver, yet this organ did not appear to have any obvious histopathological damage. DCF-AG synthesis would be high in the liver, and it is plausible that DCF-AG adducted albumin, which is synthesized in the liver, and/or

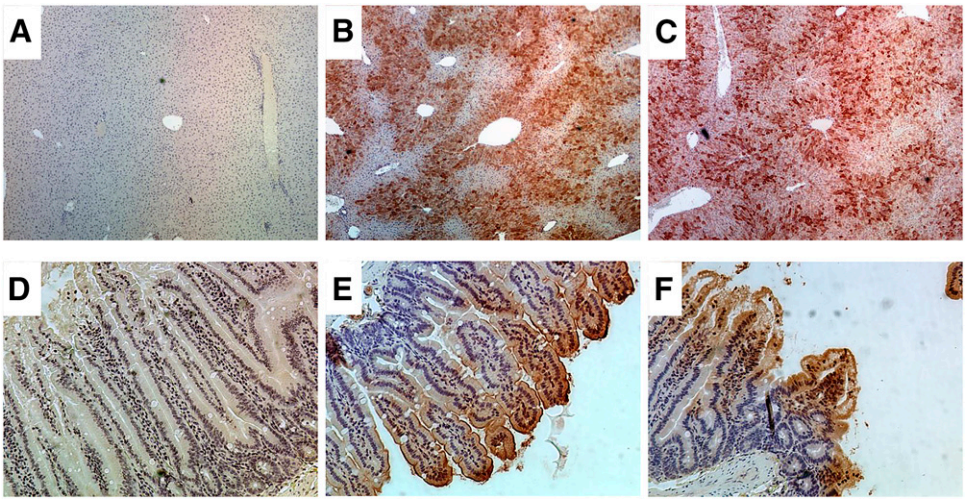

Fig. 5. Immunohistochemistry of tissues taken from C57 wild-type (WT) and C57 Mrp3-null (KO) mice treated with vehicle or 90 mg/kg DCF (immunoperoxidase with hematoxylin counterstain). Tissues were harvested 24 hours after administration. (A–C) Liver sections at 4× magnification. (A) Representative liver section from vehicle-treated subject. (B) WT liver after 90 mg/kg. (C) KO liver after 90 mg/kg. (D–F) Small intestine sections at 15× magnification. (D) Representative small intestine from vehicle treated subject. (E) WT small intestine after 90 mg/kg. (F) KO small intestine after 90 mg/kg. The presence of DCF adducts is visualized by the presence of red/brown staining.

DCF-AG was sequestered by thiols (protein and nonprotein) that are not critical cellular targets. Although staining in small intestines was less robust, histopathology revealed significant damage (Fig. 4). DCF-AG adduction to enterocytes potentially compromised enterocyte function and viability and possibly induced an immune-mediated response. Modulation of the immune function within 24 hours of toxicant exposure has previously been demonstrated for drugs such as acetaminophen. Administration of a toxic acetaminophen dose activates hepatic macrophages (i.e., Kupffer cells) to release proinflammatory cytokines (Blazka et al., 1995). This in turn stimulates the migration and infiltration of immune cells into the liver, influencing the ultimate toxic outcome. The role of the immune system in intestinal toxicity after DCF administration was beyond the scope of the present work and will be a focus of future studies.

DCF-AG could adduct enterocyte proteins on the extracellular surface or alternatively adduct from within after uptake by various transporters. Glucuronide conjugates can be transported by organic anion transporting polypeptides (OATPs) of which OATP2B1 is the predominant isoform in the human intestine (Ishiguro et al., 2008; Drozdzik et al., 2014). It is likely through the mouse Oatp2b1 ortholog, which is also expressed in the intestines, that DCF-AG uptake occurs (Cheng et al., 2005). Nonetheless, the fact that the liver had intense adduct formation without apparent injury compared with the intestine, which had extensive damage but moderate adduction, may indicate that protein adducts of DCF metabolite(s) do not necessarily contribute to or cause toxicity.

DCF administration resulted in two diverse outcomes: (1) rapid generation of DCF-AG that was excreted into bile or plasma and (2) COX inhibition that decreased local and/or systemic prostaglandins that protect the GI mucosa. Based on the data, we propose the following series of events to occur in our model of DCF-induced toxicity. DCF-AG is taken up and covalently binds to targets (plasma membrane, intracellular proteins, etc.), compromising the integrity of the enterocyte. In KO, the DCF-AG basolateral efflux is attenuated, potentially leading to higher accumulation of intracellular DCF-AG within enterocytes compared with WT. Meanwhile, intestinal mucosal protection is weakened because of DCF's pharmacological inhibition of both COX-1 and COX-2 (Menasse et al., 1978), causing a decrease in protective prostaglandins. Simultaneously, the highly permeable DCF enters enterocytes and exerts further injury through mitochondrial dysfunction, leading to apoptosis (Gomez-Lechon et al., 2003; Lim et al., 2006). Unbound DCF-AG may also dissociate into DCF and glucuronic acid, intensifying diclofenac-induced mitochondrial dysfunction. Mrp2, which normally confers a measure of protection via DCF-AG efflux, could be affected as Mrp2 translocates intracellularly from its apical membrane localization during oxidative stress (Sekine et al., 2006). The proposed events would breakdown the overall intactness of the GI tract.

There are several issues that remain to be addressed: (1) the relationship between DCF-AG exposure and developing injury is unclear, (2) determining the DCF-AG concentrations in the small intestine that can cause damage, and (3) assessing why the small intestines but not liver or kidneys were affected. It will be necessary to devise experiments wherein the mechanism of injury by DCF-AG can be studied with minimal interference from its parent or hydroxylated metabolites. The degree of intestinal COX inhibition also warrants examination as a contributing cause for the GI injury observed after DCF administration.

In conclusion, the present work demonstrates that (1) Mrp3 is responsible for DCF-AG basolateral efflux, (2) canalicular efflux is not perturbed by Mrp3 deletion, (3) KO mice have greater gastrointestinal damage compared with WT, and (4) appearance of adducts does not necessarily signify the occurrence of injury as certain organs are more sensitive to injury than others.

Acknowledgments

The authors thank Drs. Lauren Aleksunes and Andrew Lickteig for assistance with pilot studies and tissue collections, Dr. Urs Boelsterli and Dr. Christopher L. Shaffer for feedback on experimental design and data, and Ms. Denise Woodard for technical support on immunohistochemistry.

Authorship Contributions

Participated in research design: Scialis, Csanaky, Manautou.
Conducted experiments: Scialis, Csanaky.
Performed data analysis: Scialis, Goedken.
Wrote or contributed to the writing of the manuscript: Scialis, Csanaky, Manautou.

References

Altschul SF, Wootton JC, Gertz EM, Agarwala R, Morgulis A, Schäffer AA, and Yu YK (2005) Protein database searches using compositionally adjusted substitution matrices. *FEBS J* **272**: 5101–5109.

Atchison CR, West AB, Balakumaran A, Hargus SJ, Pohl LR, Daiker DH, Aronson JF, Hoffmann WE, Shipp BK, and Treinen-Moslen M (2000) Drug enterocyte adducts: possible causal factor for diclofenac enteropathy in rats. *Gastroenterology* **119**:1537–1547.

Blazka ME, Wilmer JL, Holladay SD, Wilson RE, and Luster MI (1995) Role of proinflammatory cytokines in acetaminophen hepatotoxicity. *Toxicol Appl Pharmacol* **133**:43–52.

Cheng X, Maher J, Chen C, and Klaassen CD (2005) Tissue distribution and ontogeny of mouse organic anion transporting polypeptides (Oatps). *Drug Metab Dispos* **33**:1062–1073.

Daly AK, Aithal GP, Leathart JB, Swainsbury RA, Dang TS, and Day CP (2007) Genetic susceptibility to diclofenac-induced hepatotoxicity: contribution of UGT2B7, CYP2C8, and ABCC2 genotypes. *Gastroenterology* **132**:272–281.

de Abajo FJ, Montero D, Madurga M, and García Rodríguez LA (2004) Acute and clinically relevant drug-induced liver injury: a population based case-control study. *Br J Clin Pharmacol* **58**:71–80.

Depomed (2009) Cambia (diclofenac potassium for oral solution) prescribing information. Newark, CA

Drozdzik M, Gröer C, Penski J, Lapczuk J, Ostrowski M, Lai Y, Prasad B, Unadkat JD, Siegmund W, and Oswald S (2014) Protein abundance of clinically relevant multidrug transporters along the entire length of the human intestine. *Mol Pharm* **11**:3547–3555.

Ebner T, Heinzel G, Prox A, Beschke K, and Wachsmuth H (1999) Disposition and chemical stability of telmisartan 1-O-acylglucuronide. *Drug Metab Dispos* **27**:1143–1149.

Fukushima-Uesaka H, Saito Y, Maekawa K, Hasegawa R, Suzuki K, Yanagawa T, Kajio H, Kuzuya N, Noda M, and Yasuda K, et al. (2007) Genetic variations of the ABC transporter gene ABCC3 in a Japanese population. *Drug Metab Pharmacokinet* **22**:129–135.

Gómez-Lechón MJ, Ponsoda X, O'Connor E, Donato T, Castell JV, and Jover R (2003) Diclofenac induces apoptosis in hepatocytes by alteration of mitochondrial function and generation of ROS. *Biochem Pharmacol* **66**:2155–2167.

Hargus SJ, Martin BM, George JW, and Pohl LR (1995) Covalent modification of rat liver dipeptidyl peptidase IV (CD26) by the nonsteroidal anti-inflammatory drug diclofenac. *Chem Res Toxicol* **8**:993–996.

Hickey EJ, Raje RR, Reid VE, Gross SM, and Ray SD (2001) Diclofenac induced in vivo nephrotoxicity may involve oxidative stress-mediated massive genomic DNA fragmentation and apoptotic cell death. *Free Radic Biol Med* **31**:139–152.

Huang L, Berry L, Ganga S, Janosky B, Chen A, Roberts J, Colletti AE, and Lin MH (2010) Relationship between passive permeability, efflux, and predictability of clearance from in vitro metabolic intrinsic clearance. *Drug Metab Dispos* **38**:223–231.

Ishiguro N, Maeda K, Saito A, Kishimoto W, Matsushima S, Ebner T, Roth W, Igarashi T, and Sugiyama Y (2008) Establishment of a set of double transfectants coexpressing organic anion transporting polypeptide 1B3 and hepatic efflux transporters for the characterization of the hepatobiliary transport of telmisartan acylglucuronide. *Drug Metab Dispos* **36**:796–805.

Kenny JR, Maggs JL, Meng X, Sinnott D, Clarke SE, Park BK, and Stachulski AV (2004) Syntheses and characterization of the acyl glucuronide and hydroxy metabolites of diclofenac. *J Med Chem* **47**:2816–2825.

King C, Tang W, Ngui J, Tephly T, and Braun M (2001) Characterization of rat and human UDP-glucuronosyltransferases responsible for the in vitro glucuronidation of diclofenac. *Toxicol Sci* **61**:49–53.

Kobayashi K, Ito K, Takada T, Sugiyama Y, and Suzuki H (2008) Functional analysis of non-synonymous single nucleotide polymorphism type ATP-binding cassette transmembrane transporter subfamily C member 3. *Pharmacogenet Genomics* **18**:823–833.

Kretz-Rommel A and Boelsterli UA (1993) Diclofenac covalent protein binding is dependent on acyl glucuronide formation and is inversely related to P450-mediated acute cell injury in cultured rat hepatocytes. *Toxicol Appl Pharmacol* **120**:155–161.

Krieglstein CF, Anthoni C, Cerwinka WH, Stokes KY, Russell J, Grisham MB, and Granger DN (2007) Role of blood- and tissue-associated inducible nitric-oxide synthase in colonic inflammation. *Am J Pathol* **170**:490–496.

Lagas JS, Sparidans RW, Wagenaar E, Beijnen JH, and Schinkel AH (2010) Hepatic clearance of reactive glucuronide metabolites of diclofenac in the mouse is dependent on multiple ATP-binding cassette efflux transporters. *Mol Pharmacol* **77**:687–694.

Lagas JS, van der Kruijssen CM, van de Wetering K, Beijnen JH, and Schinkel AH (2009) Transport of diclofenac by breast cancer resistance protein (ABCG2) and stimulation of multidrug resistance protein 2 (ABCC2)-mediated drug transport by diclofenac and benzbromarone. *Drug Metab Dispos* **37**:129–136.

Lang T, Hitzl M, Burk O, Mornhinweg E, Keil A, Kerb R, Klein K, Zanger UM, Eichelbaum M, and Fromm MF (2004) Genetic polymorphisms in the multidrug resistance-associated protein 3 (ABCC3, MRP3) gene and relationship to its mRNA and protein expression in human liver. *Pharmacogenetics* **14**:155–164.

Lim MS, Lim PL, Gupta R, and Boelsterli UA (2006) Critical role of free cytosolic calcium, but not uncoupling, in mitochondrial permeability transition and cell death induced by diclofenac oxidative metabolites in immortalized human hepatocytes. *Toxicol Appl Pharmacol* **217**: 322–331.

Manautou JE, de Waart DR, Kunne C, Zelcer N, Goedken M, Borst P, and Elferink RO (2005) Altered disposition of acetaminophen in mice with a disruption of the Mrp3 gene. *Hepatology* **42**:1091–1098.

Manautou JE, Hoivik DJ, Tveit A, Hart SG, Khairallah EA, and Cohen SD (1994) Clofibrate pretreatment diminishes acetaminophen's selective covalent binding and hepatotoxicity. *Toxicol Appl Pharmacol* **129**:252–263.

McNeely W and Goa KL (1999) Diclofenac-potassium in migraine: a review. *Drugs* **57**: 991–1003.

Menassé R, Hedwall PR, Kraetz J, Pericin C, Riesterer L, Sallmann A, Ziel R, and Jaques R (1978) Pharmacological properties of diclofenac sodium and its metabolites. *Scand J Rheumatol Suppl* **22**:5–16.

Moolenbeek C and Ruitenberg EJ (1981) The "Swiss roll": a simple technique for histological studies of the rodent intestine. *Lab Anim* **15**:57–59.

Novartis (2011) Voltaren (diclofenac sodium enteric-coated tablets) prescribing information. East Hanover, NJ

Ramirez-Alcantara V, LoGuidice A, and Boelsterli UA (2009) Protection from diclofenac-induced small intestinal injury by the JNK inhibitor SP600125 in a mouse model of NSAID-associated enteropathy. *Am J Physiol Gastrointest Liver Physiol* **297**:G990–G998.

Riess W, Stierlin H, Degen P, Faigle JW, Gérardin A, Moppert J, Sallmann A, Schmid K, Schweizer A, and Sulc M, et al. (1978) Pharmacokinetics and metabolism of the anti-inflammatory agent Voltaren. *Scand J Rheumatol Suppl* **22**:17–29.

Sallustio BC and Holbrook FL (2001) In vivo perturbation of rat hepatocyte canalicular membrane function by diclofenac. *Drug Metab Dispos* **29**:1535–1538.

Sallustio BC, Sabordo L, Evans AM, and Nation RL (2000) Hepatic disposition of electrophilic acyl glucuronide conjugates. *Curr Drug Metab* **1**:163–180.

Sarda S, Page C, Pickup K, Schulz-Utermoehl T, and Wilson I (2012) Diclofenac metabolism in the mouse: novel in vivo metabolites identified by high performance liquid chromatography coupled to linear ion trap mass spectrometry. *Xenobiotica* **42**:179–194.

Seitz S and Boelsterli UA (1998) Diclofenac acyl glucuronide, a major biliary metabolite, is directly involved in small intestinal injury in rats. *Gastroenterology* **115**:1476–1482.

Seitz S, Kretz-Rommel A, Oude Elferink RP, and Boelsterli UA (1998) Selective protein adduct formation of diclofenac glucuronide is critically dependent on the rat canalicular conjugate export pump (Mrp2). *Chem Res Toxicol* **11**:513–519.

Sekine S, Ito K, and Horie T (2006) Oxidative stress and Mrp2 internalization. *Free Radic Biol Med* **40**:2166–2174.

Tang W, Stearns RA, Bandiera SM, Zhang Y, Raab C, Braun MP, Dean DC, Pang J, Leung KH, and Doss GA, et al. (1999) Studies on cytochrome P-450-mediated bioactivation of diclofenac in rats and in human hepatocytes: identification of glutathione conjugated metabolites. *Drug Metab Dispos* **27**:365–372.

Tian X, Swift B, Zamek-Gliszczynski MJ, Belinsky MG, Kruh GD, and Brouwer KL (2008) Impact of basolateral multidrug resistance-associated protein (Mrp) 3 and Mrp4 on the hepatobiliary disposition of fexofenadine in perfused mouse livers. *Drug Metab Dispos* **36**:911–915.

Trelle S, Reichenbach S, Wandel S, Hildebrand P, Tschannen B, Villiger PM, Egger M, and Jüni P (2011) Cardiovascular safety of non-steroidal anti-inflammatory drugs: network meta-analysis. *BMJ* **342**:c7086.

Vlaming ML, van Esch A, Pala Z, Wagenaar E, van de Wetering K, van Tellingen O, and Schinkel AH (2009) Abcc2 (Mrp2), Abcc3 (Mrp3), and Abcg2 (Bcrp1) are the main determinants for rapid elimination of methotrexate and its toxic metabolite 7-hydroxymethotrexate in vivo. *Mol Cancer Ther* **8**:3350–3359.

Wallace JL (2008) Prostaglandins, NSAIDs, and gastric mucosal protection: why doesn't the stomach digest itself? *Physiol Rev* **88**:1547–1565.

Willis JV, Kendall MJ, Flinn RM, Thornhill DP, and Welling PG (1979) The pharmacokinetics of diclofenac sodium following intravenous and oral administration. *Eur J Clin Pharmacol* **16**: 405–410.

Zamek-Gliszczynski MJ, Nezasa K, Tian X, Bridges AS, Lee K, Belinsky MG, Kruh GD, and Brouwer KL (2006) Evaluation of the role of multidrug resistance-associated protein (Mrp) 3 and Mrp4 in hepatic basolateral excretion of sulfate and glucuronide metabolites of acetaminophen, 4-methylumbelliferone, and harmol in Abcc3-/- and Abcc4-/- mice. *J Pharmacol Exp Ther* **319**:1485–1491.

Zelcer N, Saeki T, Bot I, Kuil A, and Borst P (2003) Transport of bile acids in multidrug-resistance-protein 3-overexpressing cells co-transfected with the ileal Na+-dependent bile-acid transporter. *Biochem J* **369**:23–30.

Zelcer N, Saeki T, Reid G, Beijnen JH, and Borst P (2001) Characterization of drug transport by the human multidrug resistance protein 3 (ABCC3). *J Biol Chem* **276**:46400–46407.

Zelcer N, van de Wetering K, de Waart R, Scheffer GL, Marschall HU, Wielinga PR, Kuil A, Kunne C, Smith A, and van der Valk M, et al. (2006) Mice lacking Mrp3 (Abcc3) have normal bile salt transport, but altered hepatic transport of endogenous glucuronides. *J Hepatol* **44**: 768–775.

Address correspondence to: Josè E. Manautou, University of Connecticut, Dept. of Pharmaceutical Sciences, 69 North Eagleville Road, Storrs, CT 06269-3092. E-mail: jose.manautou@uconn.edu